Published in final edited form as:
Cell. 2015 September 24; 163(1): 84–94. doi:10.1016/j.cell.2015.08.055.

Leptin-Driven Lipolysis is Mediated by Sympathetic Neuro-Adipose Connections

Wenwen Zeng[2,3,7], **Roksana M. Pirzgalska**[1,7], **Mafalda M.A. Pereira**[1], **Nadiya Kubasova**[1], **Andreia Barateiro**[1,6], **Elsa Seixas**[1], **Yi-Hsueh Lu**[2], **Albina Kozlova**[2], **Henning Voss**[5], **Gabriel G. Martins**[4], **Jeffrey M. Friedman**[2,3,8], **Ana I. Domingos**[1,8,*]

[1]Obesity Laboratory, Instituto Gulbenkian de Ciência, Oeiras, 2780-156 Portugal

[2]Laboratory of Molecular Genetics, The Rockefeller University, New York, NY10021 United States

[3]Howard Hughes Medical Institute, The Rockefeller University, New York, NY10021 United States

[4]Advanced Microscopy Unit, Instituto Gulbenkian de Ciência, Oeiras, 2780-156 Portugal

[5]Department of Radiology, Weill Cornell Medical College, New York, NY10021, USA

[6]Research Institute for Medicines (iMed.ULisboa), Faculty of Pharmacy, Universidade de Lisboa, Av. Professor Gama Pinto, 1649-003 Lisbon, Portugal

Summary

Leptin is an adipose-derived hormone that acts in the brain to promote fat-breakdown. However, the mechanism underlying the lipolytic effect of leptin has not been established. Here we demonstrate by intra-vital two-photon microscopy that sympathetic nerve fibers can envelop adipocytes. Local optogenetic stimulation of sympathetic inputs was sufficient to induce local lipolytic response with depletion of white adipose mass. Conversely, genetic ablation of sympathetic inputs onto fat pads blocked leptin-stimulated phosphorylation of hormone sensitive lipase and consequent lipolysis, as did knockouts of dopamine β-hydroxylase an enzyme required for catecholamine synthesis. Here we visualize neuro-adipose junctions and demonstrate that they are both necessary and sufficient for the induction of lipolysis in white adipose tissue, and are an efferent effector of leptin action. Direct activation of sympathetic inputs to adipose tissues could represent a strategy for the induction of fat loss that would circumvent central leptin resistance.

Introduction

White adipose tissues (WAT) serve as a storage depot for energy rich triglycerides. In times of privation, this lipid storage can be released as part of an adaptive response to the

*Correspondence: dominan@igc.gulbenkian.pt.
[7]Co-first author
[8]Co-senior author

Author Contributions

Two-photon microscopy, and optogenetics were performed by AID, RMP, and related rodent husbandry was performed by NK and ES. OPT was performed by RMP, MMAP and GGM; MRI scans were done by HV; Amira segmentation of MRI data was done by RMP and MMAP; cell cultures and neuronal explants were developed by AB and RMP. Biochemical analyses, whole body fat composition, and body weights and were performed by WZ, NK, ES, YHL and AK; AD and JF wrote the manuscript.

Europe PMC Funders Author Manuscripts

energy shortage. Lipolysis, the process of hydrolyzing stored triglycerides in adipocytes, is regulated by several G protein-coupled receptors, including adrenergic receptors, all of which activate protein kinase A (PKA) and elevate the intracellular levels of cyclic adenosine monophosphate (cAMP) (Brasaemle, 2007). PKA also phosphorylates several key target proteins, including lipid droplet-associated protein perilipin, HSL, and a set of esterases, that collectively promote the hydrolysis of triglycerides into free fatty-acids (FFA) and glycerol, which are then released into plasma to meet the energy demands of other tissues (Brasaemle, 2007). HSL is a canonical target of PKA in adipocytes and this enzyme catalyzes the conversion of diacylglycerol to monoacyl glycerol (Brasaemle, 2007).

Adipose tissue mass is homeostatically controlled by an endocrine loop in which leptin acts on neural circuits in the hypothalamus and elsewhere in brain to regulate food intake and peripheral metabolism. In wild type (WT) and leptin-deficient *ob* animals, leptin treatment reduces food intake and leads to a rapid depletion of fat mass (Halaas et al., 1995, 1997; Montez et al., 2005). Of note, the depletion of fat mass after leptin treatment is distinct from that observed after food restriction in a number of respects: leptin treatment spares lean body mass and also potently stimulates glucose metabolism, while starvation results in a loss of lean body mass and causes insulin resistance (Newman and Brodows, 1983; Koffler and Kisch, 1996; Awad et al., 2009; Elia et al., 1999). In addition, leptin deficient *ob/ob* mice pair-fed to leptin-treated *ob* mice lose only half the weight of those treated with leptin, further implicating a mechanism beyond a reduced food intake (Rafael and Herling, 2000). Because leptin has been shown to increase the sympathetic efferent signal to brown adipose tissues (BAT) (Scarpace and Matheny, 1998; Rezai-Zadeh and Munzberg, 2013), it has been suggested that leptin also activates sympathetic efferents to white adipose tissue to increase lipolysis in WAT. However, this has not been directly shown and the nature of the effector mechanism underlying leptin-stimulated lipolysis in WAT has not been defined. In particular, it has not been established whether the increased lipolysis in white adipose tissue in response to leptin is due to a circulating hormone(s) such as norepinephrine (NE) and/or another mediator that is released either centrally or peripherally (adrenal gland or macrophages), or specific efferent neural inputs to WAT, which mediate central leptin action. However, the effect of leptin on energy balance does not require the presence of intact adrenals suggesting that this organ is unlikely to be the source of the lipolytic signal (Arvaniti et al., 1998).

While numerous previous studies have shown dense neural innervation of BAT both functionally and anatomically, the innervation of WAT has been difficult to visualize. It has thus been suggested that neural inputs to WAT are either very sparse, or difficult to be distinguished from *en passant* axons with terminals on other cell types, such as those in vasculature (Bartness et al., 2005; Bartness and Song, 2007; Youngstrom and Bartness, 1995; Giordano et al., 1996). Indeed, some reports have suggested that the only innervation of WAT is perivascular, and that white adipocytes themselves are not directly innervated (Giordano et al., 2005). This controversy has heightened the uncertainty as to the relative roles of sympathetic neural activity to regulate WAT metabolism. Alternatively, macrophages in adipose tissue account for about 10 % of the stromal vascular fraction (SVF), hence local catecholamines produced by these cells could also contribute to lipolysis in WAT *in vivo* (Weissberg et al., 2003; Nguyen et al., 2011). Thus, the dramatic decrease

of adipose tissue mass observed after leptin treatment could, in principle, be mediated by catecholamines or other mediators that are either locally produced or produced by neurons.

In this study, we use anatomic, optogenetic, biochemical, and genetic approaches to show that the catecholamines released at heretofore unidentified neuro-adipose junctions mediates the lipolytic effect of leptin, thus establishing the effector mechanism underlying depletion of fat mass by leptin, and potentially other stimuli. Our data demonstrate that the local sympathetic activity in WAT is necessary and sufficient for the lipolytic effect of leptin. In addition, genetic evidence shows that the β- but not α-adrenergic receptors partially constitute a signaling pathway that accounts for the lipolytic effect of leptin. Moreover, the effect of pre-synaptic manipulations, such as neural gain of function or loss of function, is more profound than that of post-synaptic manipulations, thus suggesting direct activation of sympathetic inputs to adipose tissues as a strategy for the induction of fat loss.

Results

Phosphorylation of HSL in WAT as a Lipolysis Marker for Leptin Action

To directly assess the cellular effect of leptin on lipolysis in white adipocytes and provide a marker for leptin action, we searched for biochemical responses in white adipocytes that were specifically activated by leptin treatment. We used a battery of phospho-specific antibodies and found that the phosphorylation of HSL was robustly increased in adipose tissue in response to leptin treatment. Note, our ability to define a biochemical effect of leptin is dependent on the quality of the antibodies and we found that the anti-pHSL antibody was extremely robust. As shown, peripheral administration of leptin led to a significant increase of phosphorylated HSL (p-HSL) in WAT that could be visualized by immunohistochemistry (Figure 1 A), and quantified by immunoblot analysis (Figure 1 B). We set out to investigate whether the effect of leptin to increase HSL phosphorylation was mediated by neural efferent outputs onto WAT.

Axonal Bundles Project to WAT and Form Sympathetic Neuro-Adipose Junctions

We first used tomography methods to determine whether fat pads were innervated. By coupling optical projection tomography (OPT) to a fat clearing method that renders whole organs transparent, we were able to macroscopically visualize and document the nerve bundles that innervate the inguinal fat pad (Figure 2 A, Experimental Procedures and Supplemental Experimental Procedures for details) (Gualda et al., 2013, Quintana and Sharpe, 2011). A full series of projections of the whole organ are acquired from multiple angles, typically 800-1600 angles, and from this series of projections a stack of axial slices can be visualized through back-projection reconstruction (Figure 2 B). From an OPT series of coronal optical sections of inguinal fat organ we performed a 3-D reconstruction, which enabled the visualization of thick axon bundles targeting the fat pad (Figure 2 C, D). Axon bundles can be identified based on the grey threshold level and morphological features that distinguish them from the vasculature (Figure 2 E). These structures within the fat were then segmented using semi-automated software (see Experimental Procedures).

The neural bundles were micro-dissected from the subcutaneous fat pads and subjected to immunostaining for tyrosine hydroxylase (TH), a marker of sympathetic neurons, and β3-tubulin (Tub-3), a general marker for the peripheral nervous system (PNS) (Figure 3 A). We found that overall ~ 50 % of the Tub-3-positive neurons also expressed TH, thus establishing the presence of both catecholaminergic and non-catecholaminergic axons innervating subcutaneous fat pads (Figure 3 A). We then used multi-photon microscopy on the intact inguinal WAT of a living mouse to visualize sympathetic neuro-adipose connections (see Experimental Procedures and Figure 3 B, C). We labeled adipocytes with LipidTOX, a lipophylic dye, and sympathetic axons by crossing TH Cre-recombinase mice (*TH-Cre*) with a Tdtomato-reporter line (*Rosa26-LSL-Tdtomato*) (Figure 3 C). We observed Tdtomato-positive axons in fat pads made dense contacts with adipocytes through bouton-like structures that had the anatomic appearance of neuro-adipocyte junctions, resembling synapses (Figure 3 C). We quantified these from 8 independent 2-photon micrographs, and determined that 8 ± 4.6 % of adipocytes are in direct contact with sympathetic nerves.

Optogenetic Stimulation of Sympathetic Inputs to WAT Leads to Catecholamine release, HSL Phosphorylation, and Fat Mass Depletion

We assessed the function of the catecholaminergic fibers by crossing the *TH-Cre* mice to a channelrhodopsin (ChR2) reporter line, *Rosa26-LSL-ChR2-YFP*. ChR2-YFP showed a complete co-localization with the endogenous TH as determined by immunostaining of YFP and TH (Figure 4 A). ChR2-YFP-expressing axons that projected onto subcutaneous WAT were then optogenetically activated using a subcutaneously implanted optical fiber targeting the right inguinal fat depot (see Experimental Procedures for surgical details).

While optogenetic tools have been widely used in the central nervous system (CNS), it has not been used as frequently to probe the function of peripheral cells including sympathetic neurons. We began by validating the use of optogenetic stimulation of sympathetic neurons in primary cultures of superior cervical ganglia (SCG) of *TH-Cre* X *Rosa26-LSL-ChR2-YFP* mice; SCG can be dissected with less difficulty compared to other sympathetic ganglia (see Supplemental Experimental Procedures for culture details). We found that optogenetic stimulation of cultured sympathetic neurons increased expression of cFos, a marker for neuronal activity, in TH-positive cells and significantly stimulated NE release *ex vivo* as assayed with ELISA (Figure 4 B, C). NE release of ChR2-positive neurons was significantly higher relative to that of ChR2-negative cells (749.6 ± 170.1 pg/ml vs. 4.8 ± 1.7 pg/ml, *p<0.05, Figures 4 B, C - see Experimental Procedures for culture and stimulation details).

We next stimulated ChR2-YFP-expressing axons *in vivo* unilaterally by placing optical fibers subcutaneously, aiming at inguinal fat pad located in the supra-pelvic flank of *TH-Cre* X *Rosa26-LSL-ChR2-YFP* mice (see Experimental Procedures for stimulation details). Activation of the ChR2-positive axons in subcutaneous WAT led to a significant increase of NE in the stimulated fat pad, relative to the contralateral un-stimulated control side (2.7 ± 0.5 vs. 1.1 ± 0.2, *p<0.05, Figure 4 D). We also observed a significant increase of HSL phosphorylation of fat on the side ipsilateral to the optical fiber, compared to the contralateral un-stimulated side (Figure 4 E). These data show that local activation of catecholaminergic inputs to fat could locally mimic the biochemical effect of leptin (Figure

4 D, E). We then tested whether a more prolonged (4 weeks) optogenetic stimulation of ChR2-positive neurons in WAT could deplete fat mass (Figure 4 F). The optical stimulation protocol was set to deliver light for every other second at 20 Hz, and the volume of subcutaneous WAT was determined using magnetic resonance imaging (MRI) with 3D reconstruction (Figure 4 F, G - see Experimental Procedures for details). After chronic activation, the size of the optogenetically stimulated ipsilateral fat pads of *TH-Cre*; *Rosa26-LSL-ChR2-YFP* mice was 23 ± 3.4 % that of the contralateral control side, representing a statistically and biologically significant decrease in fat mass (Figure 4 F, G, ****$p<0.0001$). This effect depended on ChR2 expression, as the fat pad volume of stimulated fat pads in ChR2-negative mice was unchanged (86 ± 4.3 % of the size of contralateral control fat pad) ruling out potential nonspecific effect of laser stimulation (Figure 4 G, see Experimental Procedures for details). Together, the results provide anatomical and functional evidence that there are synapse-like sympathetic inputs onto white adipocytes, and that their activation is sufficient to promote local NE release, HSL phosphorylation, and a reduction in the mass of an adipose tissue depot.

Local Sympathetic Inputs are Required for Leptin-stimulated HSL Lipolysis in WAT

Similarly to optogenetic stimulation of sympathetic innervation in white fat, leptin treatment led to an increase in NE levels in the subcutaneous adipose organ. NE levels in white adipose tissues dissected from leptin treated animals were significantly higher than in controls (78.7 ± 16.8 pg NE/ ug of protein vs. 30.7 ± 4.1 pg NE/ ug of protein, *$p<0.05$, Figure 5 A). Interestingly, leptin treatment did not affect serum NE levels (Figure 5 B) indicating that leptin locally increases NE release in white fat, but not systemically.

We next evaluated whether sympathetic activation is necessary for leptin-stimulated lipolysis by disrupting the neural inputs in WAT using pharmacologic blockade or local genetic ablation. First, we observed that administration of hexamethonium, a non-depolarizing anti-cholinergic ganglion blocker, significantly decreased the leptin-stimulated phosphorylation of HSL in adipose tissue (Figure 5 C). However, as the action of hexamethonium is systemic and is not cell type specific, affecting all ganglionic transmission, we took a complementary approach by introducing a local neural crush injury to the fibers innervating epididymal fat pads. Because of the anatomy of the fat pad, nerve fibers in the distal portion of the tissues can be efficiently eliminated by a surgical crush of the perivascular axons running parallel to the main vessels (see Experimental Procedures). We carried out physical denervation with a forcep crushing the fibers 2 mm from the distal tip for 30 seconds. Leptin was delivered 3 days post surgery through osmotic pump for 2 days. Consistent with the effect of hexamethonium, after a crush injury to the local nerve, leptin treatment failed to increase HSL phosphorylation on the denervated side compared to the intact contralateral control (Figure 5 D). This showed that local neural activation to WAT is required for the biochemical changes associated with leptin treatment.

To confirm that leptin-mediated lipolysis is the result of activation of sympathetic neural outputs to fat, we ablated these neurons by crossing the *TH-Cre* line with the diphtheria toxin receptor (DTR) mice - *Rosa26-LSL-DTR*, and injected diphtheria toxin (DT) locally in subcutaneous inguinal WAT (Buch et al., 2005). Local treatment with DT eliminated only

those sympathetic axons in the regions of the injection site, without effects on other local neuronal populations as shown by the sparing TH-negative Tub-3 positive axons at the site of injection (Figure 5 E, **p<0.001, see Supplemental Experimental Procedures for details). These injections were administered peripherally at low doses (10 ng/g) to ensure that the effect was local and to also spare TH-positive neurons in CNS (Figure S1, Domingos et al., 2013). Genetic ablation of sympathetic input to adipose tissue completely blocked the effect of leptin on HSL phosphorylation on the ipsilateral compared to the contralateral untreated side (Figure 5 F). Together, these results demonstrate that activation of sympathetic neurons in fat is necessary for leptin to stimulate HSL phosporylation in adipose tissue.

β-Adrenergic Signaling Influences Leptin-stimulated Lipolysis in WAT

Consistent with a sympathetic mechanism for the leptin mediated stimulation of lipolysis, systemic administration of the β-adrenergic agonist isoproterenol resulted in the rapid induction of p-HSL. As previously reported, isoproterenol also increased FFA release from WAT *in vitro* and *in vivo* (Figure S2). We thus set out to test whether β-adrenergic signaling was required for leptin-stimulated lipolysis.

We first examined the lipolytic response to leptin in mice with a knockout (KO) of dopamine β-hyroxylase (*DBH*), a key enzyme in the synthesis of NE and epinephrine from dopamine (Figure 6). After peripheral administration of leptin, there was a dramatic increase of HSL phosphorylation in WAT in the WT or $DBH^{+/+}$ animals, but a markedly diminished response in the $DBH^{-/-}$ littermates (Figure 6 A). Consistent with this, the total fat composition dramatically decreased in the WT mice treated with leptin, while there was only a slight change of fat mass in mice with the DBH deletion (*p<0.05, Figure 6 B). Also consistent with a diminished lipolytic effect of leptin, there was also a lower amount of weight loss in the $DBH^{-/-}$ mice (Figure 6 C). After two days of leptin treatment body weight of wild type mice decreased more than 6 % while the weight loss of $DBH^{-/-}$ was less than 2 % (*p<0.05). The data suggests that catecholamines contribute to more than 50 % of leptin's effect on body weight. Altogether, the results confirm that catecholamines are required for the leptin-stimulated lipolysis and HSL phosphorylation in WAT.

To test whether the action of leptin to drive lipolysis is mediated through β-adrenergic signaling, we crossed the β1/β2 double KO to β3 KO to generate animals with a deletion of all three β-adrenergic receptors (Figure 7). Animals with a deletion of all the three isoforms of β-adrenergic receptors showed significantly decreased HSL phosphorylation after leptin treatment in comparison to the double KO controls (Figure 7 A). However, this decrease was not as marked as that seen in individual depots after local ablation of sympathetic fibers using DT (see Figure 5 D). While leptin treatment significantly decreased total fat mass in $\beta1^{-/-}\beta2^{-/-}$ mice, this effect was significantly reduced in $\beta1^{-/-}\beta2^{-/-}\beta3^{-/-}$ triple knockout mice (Figure 6B Paired ANOVA *post hoc* test *p<0.01, comparing $\beta1^{-/-}\beta2^{-/-}\beta3^{-/-}$ with $\beta1^{-/-}\beta2^{-/-}\beta3^{+/+}$ mice after leptin treatment). In contrast, α-adrenergic receptors appeared to play only a minor role in the leptin-stimulated loss of fat mass, because α-adrenergic blockers phentolamine (5 mg/kg, IP) and phenoxybenzamine (10 mg/kg IP) failed to diminish the catabolic responses to leptin treatment in $\beta1^{-/-}\beta2^{-/-}\beta3^{+/+}$ control mice or $\beta1^{-/-}\beta2^{-/-}\beta3^{-/-}$ mice (Figure 7 C). There was also a small suppression of body weight loss in response to leptin

in the $\beta 1^{-/-}\beta 2^{-/-}\beta 3^{-/-}$ mice (Figure 7 D). These results showed that the β-adrenergic receptors are only partially necessary for leptin-mediated lipolysis of WAT, but the magnitude of the effect of a loss of β-adrenergic signaling is not as great as that observed by interfering with local neural outputs, thus suggesting that there could also be other neural mediators or interacting receptors on adipocytes (Figure 5).

Discussion

Leptin is known to stimulate lipolysis and reduce fat mass though the physiologic mechanisms responsible for this have not been fully delineated. In this study, we present data employing functional, anatomic, biochemical and genetic approaches to show that leptin increases lipolysis via the actions of sympathetic neuronal efferents to adipose tissue. These data also provide molecular, cellular and anatomic evidence confirming the existence of neuronal projections onto adipocytes, which have been the subject of conjecture but which have not been directly visualized.

The existence of neuro-adipose junctions in WAT had been inferred based on the fact that a pseudorabies retrograde tracing virus can visualize a set of neural projections in the brain (Bartness and Song, 2007). In addition, immunohistochemistry and immunofluorescence have been used to visualize contacts between sympathetic neurons and adipocytes in sliced tissue (Giordano et al., 1996; Giordano et al., 2005; Thompson, 1986). However, these methods, which require tissue slicing and fixation, do not distinguish *en passant* neurons from those that directly project onto adipocytes. The visualization of adipocyte-projecting neurons that can completely envelop an adipocyte has not been accomplished so far. We were able to directly visualize neural termini onto adipocytes using intra-vital multiphoton microscopy, which allows deep penetrance onto the live intact tissue, allowing us to visualize deeper structures without the perturbations associated with classical histological methods, which in past studies may have compromised the integrity of the neuro-adipose termini (Helmchen and Denk, 2005).

Confocal or multiphoton microscopy methods are suitable for histological analysis at a microscopic spatial scale, but do not give a 3-dimensional perspective of the organization of the organ as a whole. At a macroscopic spatial scale, methods such as MRI or computed tomography (CT) allow for measurement of whole body fat distribution. However, all of these methods lack the spatial resolution that is required for visualizing structures such as nerve bundles. OPT is a technique with physical principles similar to X-ray CT/gamma radiation, which uses visible light instead of radiation (Gualda et al., 2013.). Scattering of light passing through tissues is minimized by clearing lipids from the whole organ (Quintana and Sharpe, 2011). Unlike most currently available methods, OPT coupled to tissue clearing allows imaging of whole-mount samples with a spatial scale in the order of centimeters.

It has been previously shown that electrical stimulation of WAT nerve bundles can drive lipolysis (Correll, 1963). However, as shown here, nerve bundles in WAT have mixed molecular identity, making it difficult to ascertain the identity of the neurons responsible for this effect. To address this limitation we employed optogenetics, which allows for cell specific stimulation of neurons and in the current studies was used to specifically

activate sympathetic neurons in *TH-Cre* mice (Domingos et al., 2011; Domingos et al., 2013). Another advantage of this approach is that it enables the specific activation of axonal projections and, does not require stimulation of neuronal cell bodies (Petreanu et al., 2007; Vrontou et al., 2013). This feature is particularly convenient for autonomic neurons, given the deep localization of their cell bodies along the anterior face of the spinal cord and the intrinsic difficulty of implanting optical fibers in this location. Previous studies using neural tracing have revealed that sympathetic neurons innervating the subcutaneous inguinal fat pads localize to the 13^{th} thoracic ganglia, which localizes at the dorsal edge of the diaphragm muscle, in the transition between the thorax and the abdomen (Youngstrom and Bartness, 1995). This anatomical location is particularly inaccessible and unsuitable for chronic implants of optical fibers or equivalent devices. However, as we show here, subcutaneous implant of optical fibers for stimulation of nerve terminals is feasible and effective. We used this approach to show that optogenetic gain of function of the catecholaminergic signaling to the neuro-adipose junction can lead to the phosphorylation of HSL and lipolysis of WAT. Similarly, previous loss of function experiments that assessed the effect of sympathetic input on lipolysis also did not allow analysis of the effect of specific cells in the way that optogenetics can. Thus, the use of mechanical denervation, does not distinguish between neurons that directly innervate adipocytes versus those that are passing through. We have not yet profiled the non-TH nerve fibers but it is reasonable to expect that some might be parasympathetic, nociceptive, sensory fibers and/or *en passant* axons. The function of these fibers could be assessed similarly to those that we report using optogenetics to activate other populations including cholinergic neurons by studying choline acetyltransferase (ChAT)-Cre mice and/or neurons expressing other molecular markers. Chemical ablation with capsaicin also has limitations, as this treatment is not specific to sympathetic neurons and affects all transient receptor potencial vaniloid (TRPV)-expressing fibers (Holzer, 1991). Chemical ablation with 6-hydroxydopamine is likely to affect dopaminergic as well as enteric neurons, creating secondary systemic effects (Ding et al., 2004).

To avoid these limitations and gain local control over sympathetic neural activity, we used additional molecular genetic tools that combine tissue-specificity with a localized effect. We show that ablation of the sympathetic neurons by DTR expression in TH-positive neurons followed by local DT injection in WAT abolishes the effect of leptin on HSL phosphorylation. We also noted that the loss of function due to post-synaptic manipulations (i.e. the triple β-adrenergic receptor KO in Figure 7) has a lesser effect on the size of adipose tissue depots than that seen after pre-synaptic manipulations such as a loss of DBH, or pharmacologic or mechanical ablation of neural input to fat (Figure 6). This suggests that leptin-induced production of NE from sympathetic neurons could act through additional receptors that are not one of the three β-adrenergic receptors that we tested, as has been suggested by others (Tavarnier, 2005). Alternatively, sympathetic neurons may co-release other neurotransmitters or neuropeptides that signal through non-adrenergic receptors. This could account for the residual leptin-induced weight loss seen in $DBH^{-/-}$, although this effect is not significant when compared to controls. Thus, an in-depth knowledge of the underlying sympathetic neural circuits could provide strategies to pharmacologically activate specific

sympathetic neuronal population, thus circumventing leptin resistance, as potential treatment of obesity.

A canonical effect of leptin is to increase sympathetic signaling to BAT thus promoting the thermogenesis (Bachman et al., 2002; Landsberg et al., 1984). However the role of autonomic stimulation of white fat has been less well studied. We now show that the sympathetic activity is also responsible for the leptin-stimulated lipolysis in WAT. While leptin has been assumed to increase lipolysis via activation of sympathetic efferent fibers, this has not been directly shown. Adrenergic agonists have been shown to induce the formation of beige (brite) fat and these data suggest that sympathetic innervation may also stimulate this phenotypic change in adipose tissue (Bachman et al., 2002; Giralt and Villarroya, 2013; Dempersmier et al., 2015). Consistent with this, leptin has also been suggested to increase the formation of beige fat (Dodd et al., 2015).

Because brown adipocytes have relatively smaller fat storages compared to white adipocytes, while having higher metabolic demand, the continuous thermogenic response of BAT might require the supply of FFA from WAT mobilized in other parts of the body. It is therefore reasonable to speculate that the coordinated sympathetic actions in BAT and WAT in response to leptin could help maximize the hormone's effect on energy expenditure and fat metabolism. Future studies delineating the neural circuits connecting the central action of leptin with the peripheral activation of sympathetic system will be necessary to test this hypothesis. Particularly, it would be of great importance to develop technologies that would allow whole body visualization and mapping of peripheral neuronal circuits using some of the approaches presented here.

In summary, we provide direct evidence that the sympathetic neuro--adipose junction is both necessary and sufficient for leptin to drive lipolysis in WAT.

Experimental Procedures

Antibodies and drugs

The antibodies were obtained from the following vendors: HSL (Cellsignaling), phospho-HSL (Cellsignaling), phospho-PKA substrate (Cellsignaling), TH (Peel-freez) and actin (Sigma). Hexomethinium Choloride, phentolamine and phenoxybenzamine were from Sigma. DT was purchased from Merck Millipore. Recombinant mouse leptin was obtained from Amylin Pharmaceuticals (San Diego, CA).

Mice

DBH knockout mice were kindly provided by Steve Thomas in University of Pennsylvania. Adrβ1$^{-/-}$2$^{-/-}$ and Adrβ3$^{-/-}$ were kindly provided by Bruce Spiegelman at Harvard Medical School. *TH-Cre*, Rosa26-LSL-ChR2-YFP (Stock No. 012-569, Daou et al., 2013), Rosa26-LSL-DTR and C57BL/B6J mice at 6-10 weeks old were purchased from The Jackson Laboratory (JAX). Animal procedures were approved by the ethics committee of Instituto Gulbenkian de Ciência and IACUC of Rockefeller University.

Optical Projection Tomography (OPT)

6 weeks old C57BL/6 mice were sacrificed with carbon dioxide. The inguinal fat pads were dissected from the mice with Dumont #5 Forceps, fixed in 4 % paraformaldehyde (Sigma-Aldrich) for 3 h at room temperature (RT) and subjected to the OPT clearing protocol as described in Supplemental Experimental Procedures. Images of the whole fat tissue were acquired using a 1x lens, mounted on an Infinitube tube lens, and projected into an Hamamatsu FlashLT sCMOS camera. A total of 1600 images were acquired for a full rotation (0.25 degree steps). The series of projections were then pre-processed for back-projection using FIJI in order to remove hot pixels, re-align the axis of rotation in relation to the camera-chip, and finally the back-projection reconstruction was done using the Skyscan's NRecon software (Schindelin et al., 2012). The stack of slices was further processed with FIJI, to increase contrast and saved to posterior analysis with the software Amira V5.3. Using this software, 3D reconstructions and image segmentation was performed to identify and reconstruct individual parts of the fat organs. Detailed instructions for setting up an OPT system can be found at: https://sites.google.com/site/openspinmicroscopy/home/opt.

In vivo 2-photon microscopy

Mice 2 months old were kept anesthetized with 2% isofluorane. During surgery, body temperature was maintained at 37° C with a warming pad. After application of local anesthetics (lidocaine), a sagittal incision of the skin is made above the supra-pelvic flank to expose the subcutaneous inguinal fat pad. An imaging chamber was custom built to minimize fat movement. Warm imaging solution (in mM: 130 NaCl, 3 KCl, 2.5 $CaCl_2$, 0.6 $6H_2O$,$MgCl_2$, 10 HEPES without Na, 1.2 $NaHCO_3$, 10 glucose, pH 7.45 with NaOH) (37°C) mixed with a fat dye (LipidTOX) was applied to label adipocytes, maintain tissue integrity, and to allow the use of immersion objective. Imaging experiments were performed under a two-photon laser-scanning microscope (Ultima, Prairie Instruments Inc.). Live images were acquired at 8–12 frames per second, at depths below the surface ranging from 100 to 250 mm, using an Olympus 20x 0.8 N.A. water immersion objective, with a laser tuned to 860-940 nm wavelength, and emission filters 525/50 nm and 595/50 nm for green and red fluorescence, respectively. Laser power was adjusted to be 20–25 mW at the focal plane (maximally 35 mW), depending on the imaging depth and level of expression of dtTomato and LipidTOX spread. tdTomato fluorescence was used to identify TH-positive fibers until photo-bleaching occurred.

Leptin treatment and lipolysis analysis

To examine the effect of leptin treatment on lipolysis, leptin (delivery rate of 500 ng/h) or saline was delivered through osmotic pumps (Alzet; Palo Alto, CA) subcutaneously for 2 days. Body weight was recorded daily. Body fat composition was measured using EchoMRI body analyzer at end point before subcutaneous or epididymal adipose tissues were collected. HSL phosphorylation was detected by both immunohistochemistry of paraffin sections at 6 μm thickness and/or western blot of subcutaneous or epididymal adipose tissues. NE levels in serum and subcutaneous fad pads were determined with NE ELISA kit (Labor Diagnostika Nord GmbH, Nordhorn, Germany). Tissues were homogenized and

sonicated in homogenization buffer (1 N HCl, 1 mM EDTA) and cellular debris was pelleted by centrifugation at 13 000 r.p.m. for 15 min at 4°C. All tissue samples were normalized to total tissue protein concentration.

Mechanical denervation

The nerve bundle 2 mm distal from the tip of the epididymal fat was physically crushed for 30 seconds and then released using a forcep. Leptin was administrated through osmotic pump 3 days after nerve crush. HSL phosphorylation was detected two days upon leptin treatment.

Hexomethium chloride, isopreterenol and α-blocker treatment

Hexomethium chloride (500 μg/h) was administrated during leptin treatment through separate osmotic pump, and α-blockers, phentolamine (5 mg/kg, IP) and phenoxybenzamine (10 mg/kg IP) were administrated twice a day during the course of leptin treatment (500 ng/h). Isopreterenol (250 μg per mouse) was delivered in saline through jugular vein injection. Blood was drawn through tail bleeding and plasma free fatty acid was measured using NETO kit (Wako). For FFA release upon isopreterenol treatment *in vitro*, adipose tissue explants were dissected and cultured in Hanks medium and stimulated with isopretenerol at 10 μg/ml for 3 hours. FFA was measured in the medium.

NE measurements after optogenetic stimulation ex vivo

SCG were removed from 28-30 days old *TH-Cre* X *Rosa26-LSL-ChR2-YFP* mice under a stereomicroscope and placed in Dulbecco's Modified Eagle's medium (DMEM, Invitrogen, Carlsbad, CA, U.S.A.). Ganglia were cleaned from the surrounding tissue capsule and transferred into 8-well Tissue Culture Chambers (Sarstedt, Nümbrecht, Germany) that were previously coated with poly-D-lysine (Sigma/Aldrich, Steinheim, Germany) in accordance to the manufacturer's instructions. Ganglia were then covered with 5 μl of Matrigel (BD Bioscience, San Jose, CA, U.S.A.) and incubated for 7 min at 37 °C. DMEM without phenol red (Invitrogen) supplemented with 10 % fetal bovine serum (Invitrogen), 2 mM L-Glutamine (Biowest, Nuaillé, France) and nerve growth factor (Sigma/Aldrich) was subsequently added. SCG ganglia were cultured for minimum 24 h prior to further manipulation. Depolarization of sympathetic neurons in explant cultures was performed on a Yokogawa CSU-X Spinning Disk confocal using the 488 nm laser line and pointing at the region of interest (ROI) for 200 μs. Stimulation was repeated 5 times using 40 % of laser intensity. NE in the SCG explant culture medium was determined with NE ELISA kit (Labor Diagnostika Nord GmbH, Nordhorn, Germany). The same procedure was performed for *LSL-ChR2-YFP* control mice.

Surgeries and optogenetic stimulation

General anesthesia was induced and maintained with isofluorane. After application of local anesthetics (lidocaine), a sagittal incision of the skin was made above the neck and supra-pelvic flank. A hemostat was inserted into the incision, and, by opening and closing the jaws of the hemostat, spread the subcutaneous tissue to create a longitudinal pocket for the optical fiber. The pocket was made long enough to allow about 4-6 cm of fiber (Thor Labs FT200).

The tip of the fiber targeted the anatomical location of the inguinal fat pad. The other end of the fiber, the ferrule-connector end, was secured along the skin via sutures and dermal staples. Appropriate local analgesic was used post-surgically. Optogenetical stimulations were performed 48 hours after surgical procedures.

Stimulation session in Figure 3 D lasted 4-6 h and was done via a one second 20 Hz pulse of blue laser every other second, originating from a 473 nm solid laser source (OEM-BL-473-00100-CWM-SD-05). Laser source had an output power of 100 mW. Ferrule-coupled optical fibers of 200 um diameter (Thorlabs - FT200EMT-CANNULA - TS1031629) were connected to ferrule patch cords (Thorlabs - FT200EMT-FC/PC-ferrule) with mating sleeves (Thorlabs - ADAF1), and the later to the laser source via FC/PC adaptor.

NE in subcutaneous fad pads was determined with NE ELISA kit (Labor Diagnostika Nord GmbH, Nordhorn, Germany) as described above.

Stimulation protocol in Figure 3 E took place every day for two weeks, and solely during the rodent rest period. Longer sessions as in Figure 3 F had duration of four weeks. Stimulation sessions lasted 4-6 h and were performed as described above.

MRI fat measurements and fat pad segmentation

Mice were subjected to optogenetic stimulation as stated above, perfused with 4 % PFA/PBS, post-fixed over 2-3 days and embedded in Fomblin Oil (Sigma) for scanning. Imaging was performed on a 7.0 Tesla 70/30 Bruker Biospec small animal MRI system with a 12 cm diameter 450 mT/m amplitude and 4500 T/m/s slew rate actively shielded gradient subsystems with integrated shim capability. A linear coil with 7 cm diameter and a length sufficient to cover the whole body of the animal is used for excitation and reception of the magnetic resonance signal. Two image sets were acquired, one with fat suppression and one without. Axial images, covering the whole animal in 75 0.4 mm thick slices without gap were acquired in an interleaved way by using a RARE pulse sequence with RARE factor 2. Four averages with a flip angle of 90 degrees, TE = 10 ms, TR = 2468 ms, field of view = 10 x 3 cm, and matrix size = 256 × 128 (acquisition matrix size = 256 × 96), resulting in a spatial resolution of 0.391 × 0.234 × 0.4 mm, were acquired. The fat suppression, added to the second scan, consists of a 90 degree Gaussian pulse with 2.6067 ms duration and 1051.1 Hz bandwidth. Data was converted into TIF files by FIJI software. The subcutaneous inguinal fat distribution was determined with semi-automated Amira V5.3 software segmentation of scanned images. Amira V5.3 software segmentation relies on automated grouping of pixels with the same index of intensity in the grey-scale. An automatic segmentation based on the grey threshold levels, which decomposes the image domain into subsets, allowed to define the right and the left inguinal fat depots, which were further saved as unique fields. Volume of the right and the left subcutaneous fat pad was defined as the number of voxels times size of a single voxel. The size of stimulated fat pads was determined, and the effect of optogenetic stimulation of neurons on fat mass was calculated in the same animal relative to non-stimulated contralateral side.

Statistical methods

Statistics were performed in GraphPad Prism and involved computation of means, standard errors of the mean, which accompany each figure legends. T-tests and ANOVAS were employed where appropriate, and p values are indicated in text.

Supplementary Material

Refer to Web version on PubMed Central for supplementary material.

Acknowledgements

This work was supported by the Fundação para a Ciência e Tecnologia (FCT) grant number PTDC/BIM-MET/1604/2012, the European Molecular Biology Organization (EMBO), the Howard Hughes Medical Institute (HHMI), and the JPB Foundation. FCT supported AID, RMP, MMAP, NK, GGM, AB and ES. JPB Foundation supported the work of WZ, YHL and AK. JMF is an HHMI investigator. The authors do not have any conflict of interest.

References

Arvaniti K, Deshaies Y, Richard D. Effect of leptin on energy balance does not require the presence of intact adrenals. Am J Physiol. 1998; 275: R105–111. [PubMed: 9688967]

Awad S, Constantin-Teodosiu D, Macdonald IA, Lobo DN. Short-term starvation and mitochondrial dysfunction - a possible mechanism leading to postoperative insulin resistance. Clin Nutr. 2009; 28: 497–509. [PubMed: 19446932]

Bachman ES, Dhillon H, Zhang CY, Cinti S, Bianco AC, Kobilka BK, Lowell BB. betaAR signaling required for diet-induced thermogenesis and obesity resistance. Science. 2002; 297: 843–845. [PubMed: 12161655]

Bartness TJ, Kay Song C, Shi H, Bowers RR, Foster MT. Brain-adipose tissue cross talk. Proc Nutr Soc. 2005; 64: 53–64. [PubMed: 15877923]

Bartness TJ, Song CK. Thematic review series: adipocyte biology. Sympathetic and sensory innervation of white adipose tissue. J Lipid Res. 2007; 48: 1655–1672. [PubMed: 17460327]

Brasaemle DL. Thematic review series: adipocyte biology. The perilipin family of structural lipid droplet proteins: stabilization of lipid droplets and control of lipolysis. J Lipid Res. 2007; 48: 2547–2559. [PubMed: 17878492]

Buch T, Heppner FL, Tertilt C, Heinen TJ, Kremer M, Wunderlich FT, Jung S, Waisman A. A Cre-inducible diphtheria toxin receptor mediates cell lineage ablation after toxin administration. Nat Methods. 2005; 2: 419–426. [PubMed: 15908920]

Campfield LA, Smith FJ, Guisez Y, Devos R, Burn P. Recombinant mouse OB protein: evidence for a peripheral signal linking adiposity and central neural networks. Science. 1995; 269: 546–549. [PubMed: 7624778]

Correll JW. Adipose tissue: ability to respond to nerve stimulation in vitro. Science. 1963; 140: 387–388. [PubMed: 14023160]

Daou I, Tuttle AH, Longo G, Wieskopf JS, Bonin RP, Ase AR, Wood JN, Koninck YD, Ribeiro-da-Silva A, Mogil JS, et al. Remote Optogenetic Activation and Sensitization of Pain Pathways in Freely Moving Mice. J Neurosci. 2013; 33: 18631–18640. DOI: 10.1523/JNEUROSCI.2424-13.2013 [PubMed: 24259584]

Dempersmier J, Sambeat A, Gulyaeva O, Paul SM, Hudak CS, Raposo HF, Kwan HY, Kang C, Wong RH, Sul HS. Cold-inducible Zfp516 activates UCP1 transcription to promote browning of white fat and development of brown fat. Mol Cell. 2015; 57: 235–246. DOI: 10.1016/j.molcel.2014.12.005 [PubMed: 25578880]

Ding YM, Jaumotte JD, Signore AP, Zigmond MJ. Effects of 6-hydroxydopamine on primary cultures of substantia nigra: specific damage to dopamine neurons and the impact of glial cell line-derived neurotrophic factor. J Neurochem. 2004; 89: 776–787. [PubMed: 15086533]

Dodd GT, Decherf S, Loh K, Simonds SE, Wiede F, Balland E, Merry TL, Munzberg H, Zhang ZY, Kahn BB, et al. Leptin and insulin act on POMC neurons to promote the browning of white fat. Cell. 2015; 160: 88–104. DOI: 10.1016/j.cell.2014.12.022 [PubMed: 25594176]

Domingos AI, Sordillo A, Dietrich MO, Liu ZW, Tellez LA, Vaynshteyn J, Ferreira JG, Ekstrand MI, Horvath TL, de Araujo IE, et al. Hypothalamic melanin concentrating hormone neurons communicate the nutrient value of sugar. Elife. 2013; 2 e01462 doi: 10.7554/eLife.01462 [PubMed: 24381247]

Domingos AI, Vaynshteyn J, Voss HU, Ren X, Gradinaru V, Zang F, Deisseroth K, de Araujo IE, Friedman J. Leptin regulates the reward value of nutrient. Nat Neurosci. 2011; 14: 1562–1568. DOI: 10.1038/nn.2977 [PubMed: 22081158]

Elia M, Stubbs RJ, Henry CJ. Differences in fat, carbohydrate, and protein metabolism between lean and obese subjects undergoing total starvation. Obes Res. 1999; 7: 597–604. [PubMed: 10574520]

Friedman JM, Halaas JL. Leptin and the regulation of body weight in mammals. Nature. 1998; 395: 763–770. [PubMed: 9796811]

Giordano A, Frontini A, Murano I, Tonello C, Marino MA, Carruba MO, Nisoli E, Cinti S. Regional-dependent increase of sympathetic innervation in rat white adipose tissue during prolonged fasting. J Histochem Cytochem. 2005; 53: 679–687. [PubMed: 15928317]

Giordano A, Morroni M, Santone G, Marchesi GF, Cinti S. Tyrosine hydroxylase, neuropeptide Y, substance P, calcitonin gene-related peptide and vasoactive intestinal peptide in nerves of rat periovarian adipose tissue: an immunohistochemical and ultrastructural investigation. J Neurocytol. 1996; 25: 125–136. [PubMed: 8699194]

Giralt M, Villarroya F. White, brown, beige/brite: different adipose cells for different functions? Endocrinology. 2013; 154: 2992–3000. [PubMed: 23782940]

Gualda EJ, Vale T, Almada P, Feijo JA, Martins GG, Moreno N. OpenSpinMicroscopy: an open-source integrated microscopy platform. Nat Methods. 2013; 10: 599–600. [PubMed: 23749300]

Halaas JL, Boozer C, Blair-West J, Fidahusein N, Denton DA, Friedman JM. Physiological response to long-term peripheral and central leptin infusion in lean and obese mice. Proc Natl Acad Sci U S A. 1997; 94: 8878–8883. DOI: 10.1073/pnas.94.16.8878 [PubMed: 9238071]

Halaas JL, Gajiwala KS, Maffei M, Cohen SL, Chait BT, Rabinowitz D, Lallone RL, Burley SK, Friedman JM. Weight-reducing effects of the plasma protein encoded by the obese gene. Science. 1995; 269: 543–546. [PubMed: 7624777]

Helmchen F, Denk W. Deep tissue two-photon microscopy. Nat Methods. 2005; 2: 932–940. [PubMed: 16299478]

Holzer P. Capsaicin: cellular targets, mechanisms of action, and selectivity for thin sensory neurons. Pharmacol Rev. 1991; 43: 143–201. [PubMed: 1852779]

Landsberg L, Saville ME, Young JB. Sympathoadrenal system and regulation of thermogenesis. Am J Physiol. 1984; 247: E181–189. [PubMed: 6380306]

Montez JM, Soukas A, Asilmaz E, Fayzikhodjaeva G, Fantuzzi G, Friedman JM. Acute leptin deficiency, leptin resistance, and the physiologic response to leptin withdrawal. Proc Natl Acad Sci U S A. 2005; 102: 2537–2542. DOI: 10.1073/pnas.0409530102 [PubMed: 15699332]

Newman WP, Brodows RG. Insulin action during acute starvation: evidence for selective insulin resistance in normal man. Metabolism. 1983; 32: 590–596. [PubMed: 6341773]

Nguyen KD, Qiu Y, Cui X, Goh YP, Mwangi J, David T, Mukundan L, Brombacher F, Locksley RM, Chawla A. Alternatively activated macrophages produce catecholamines to sustain adaptive thermogenesis. Nature. 2011; 480: 104–108. DOI: 10.1038/nature10653 [PubMed: 22101429]

Pelleymounter MA, Cullen MJ, Baker MB, Hecht R, Winters D, Boone T, Collins F. Effects of the obese gene product on body weight regulation in ob/ob mice. Science. 1995; 269: 540–543. [PubMed: 7624776]

Petreanu L, Huber D, Sobczyk A, Svoboda K. Channelrhodopsin-2-assisted circuit mapping of long-range callosal projections. Nat Neurosci. 2007; 10: 663–668. [PubMed: 17435752]

Quintana L, Sharpe J. Optical projection tomography of vertebrate embryo development. Cold Spring Harb Protoc. 2011; 2011: 586–594. [PubMed: 21632785]

Rafael J, Herling AW. Leptin effect in ob/ob mice under thermoneutral conditions depends not necessarily on central satiation. Am J Physiol Regul Integr Comp Physiol. 2000; 278: R790–795. [PubMed: 10712302]

Rezai-Zadeh K, Munzberg H. Integration of sensory information via central thermoregulatory leptin targets. Physiol Behav. 2013; 121: 49–55. DOI: 10.1016/j.physbeh.2013.02.014 [PubMed: 23458626]

Scarpace PJ, Matheny M. Leptin induction of UCP1 gene expression is dependent on sympathetic innervation. Am J Physiol. 1998; 275: E259–264. [PubMed: 9688627]

Schindelin J, Arganda-Carreras I, Frise E, Kaynig V, Longair M, Pietzsch T, Preibisch S, Rueden C, Saalfeld S, Schmid B, et al. Fiji: an open-source platform for biological-image analysis. Nat Methods. 2012; 9: 676–682. DOI: 10.1038/nmeth.2019 [PubMed: 22743772]

Tavernier G, Jimenez M, Giacobino JP, Hulo N, Lafontan M, Muzzin P, Langin D. Norepinephrine induces lipolysis in beta1/beta2/beta3-adrenoceptor knockout mice. Mol Pharmacol. 2005; 68: 793–799. [PubMed: 15939797]

Thompson GE. Vascular and lipolytic responses of the inguinal fat pad of the sheep to adrenergic stimulation, and the effects of denervation and autotransplantation. Q J Exp Physiol. 1986; 71: 559–567. [PubMed: 3786657]

Vrontou S, Wong AM, Rau KK, Koerber HR, Anderson DJ. Genetic identification of C fibres that detect massage-like stroking of hairy skin in vivo. Nature. 2013; 493: 669–673. DOI: 10.1038/nature11810 [PubMed: 23364746]

Weisberg SP, McCann D, Desai M, Rosenbaum M, Leibel RL, Ferrante AW Jr. Obesity is associated with macrophage accumulation in adipose tissue. J Clin Invest. 2003; 112: 1796–1808. DOI: 10.1172/JCI19246 [PubMed: 14679176]

Youngstrom TG, Bartness TJ. Catecholaminergic innervation of white adipose tissue in Siberian hamsters. Am J Physiol. 1995; 268: R744–751. [PubMed: 7900918]

Europe PMC Funders Author Manuscripts

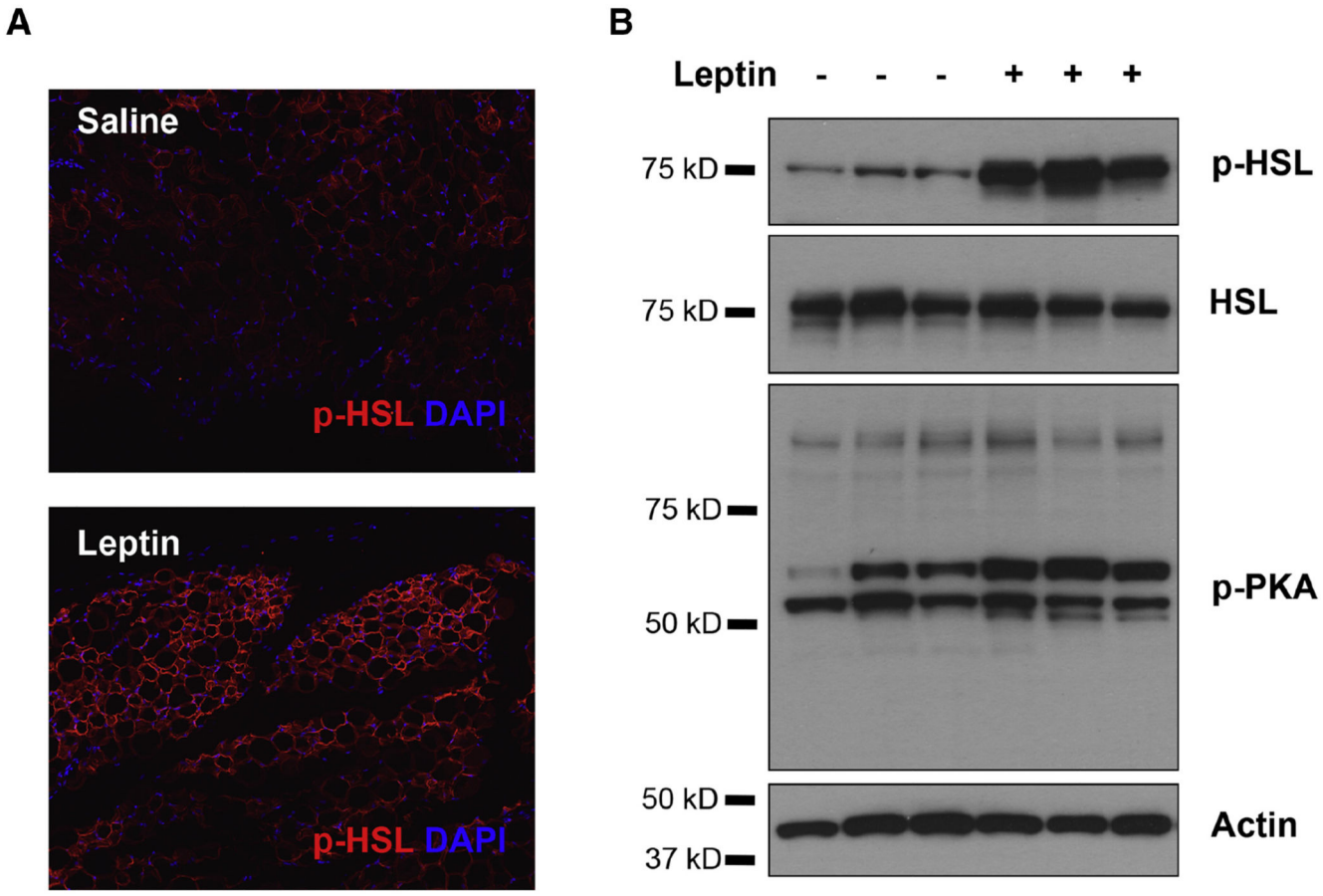

Figure 1. Leptin Stimulates HSL Phosphorylation in WAT.

(A) Immunostaining of phosphorylated HSL (red) in paraffin sections of epididymal fat of C57Bl6/J mice that were peripherally administrated with 500 ng/h recombinant leptin for 2 days. (B) Phosphorylated HSL and phosphorylated PKA substrates in total protein extracts of epididymal fats were examined by immunoblot analysis.

Europe PMC Funders Author Manuscripts

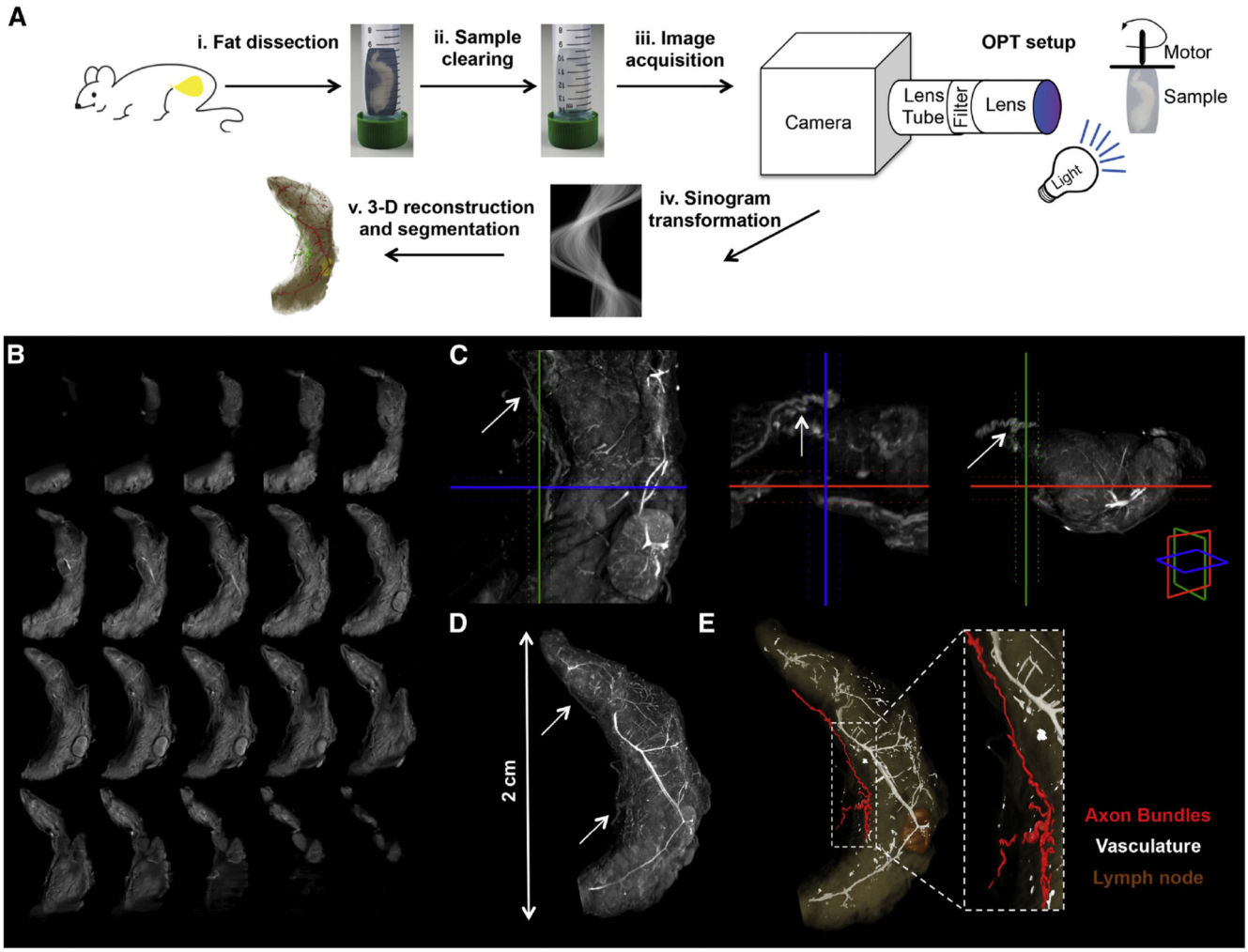

Figure 2. Neural Projections in Fat Detected with Optical Projection Tomography.

(A) Schematic representation of the OPT method applied to the subcutaneous inguinal fat. (i) Tissue dissection. (ii) Sample clearing. (iii) Image acquisition. (iv) Sinogram transformation. (v) 3-D reconstruction and segmentation. (B) OPT series of coronal sections of inguinal fat organ after 3-D reconstruction. (C) Orthogonal 400 μm OPT-slabs of inguinal fat in coronal, axial and sagittal view. Axon budles were identified based on the grey threshold level (arrows). (D) 3-D reconstruction in maximal intensity projection of the OPT coronal sections. (E) Surface view of segmented structures within inguinal fat.

Europe PMC Funders Author Manuscripts

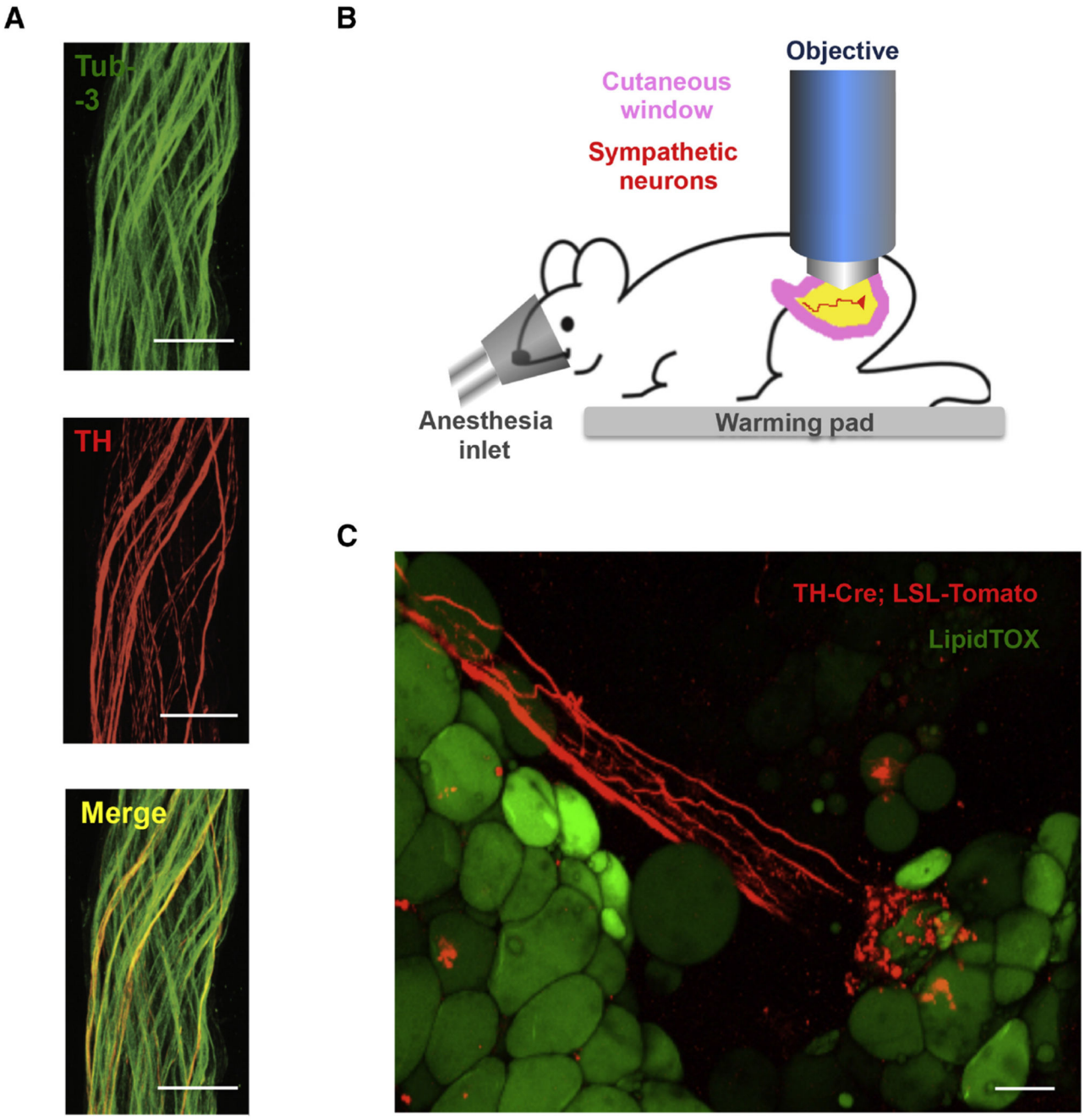

Figure 3. Catecholaminergic Neurons Innervating Adipocytes Integrate Nerve Bundles of Mixed Molecular Identity.

(A) Partial co-localization of TH (red), an SNS marker, and Tub-3 (green), a general PNS marker, shown by immunohistochemistry of nerve bundles dissected from the inguinal fat pads of WT mice. Scale bar = 50 μm. (B) Schematic representation of the two-photon intra-vital imaging of neurons in the inguinal fat pad. (C) Intra-vital two-photon microscopy visualization of a neuro-adipose connection in the inguinal fat pad of a live *TH-Cre; LSLS-Tomato* mouse – LipidTOX (green) labels adipocytes. Scale bar = 100 μm.

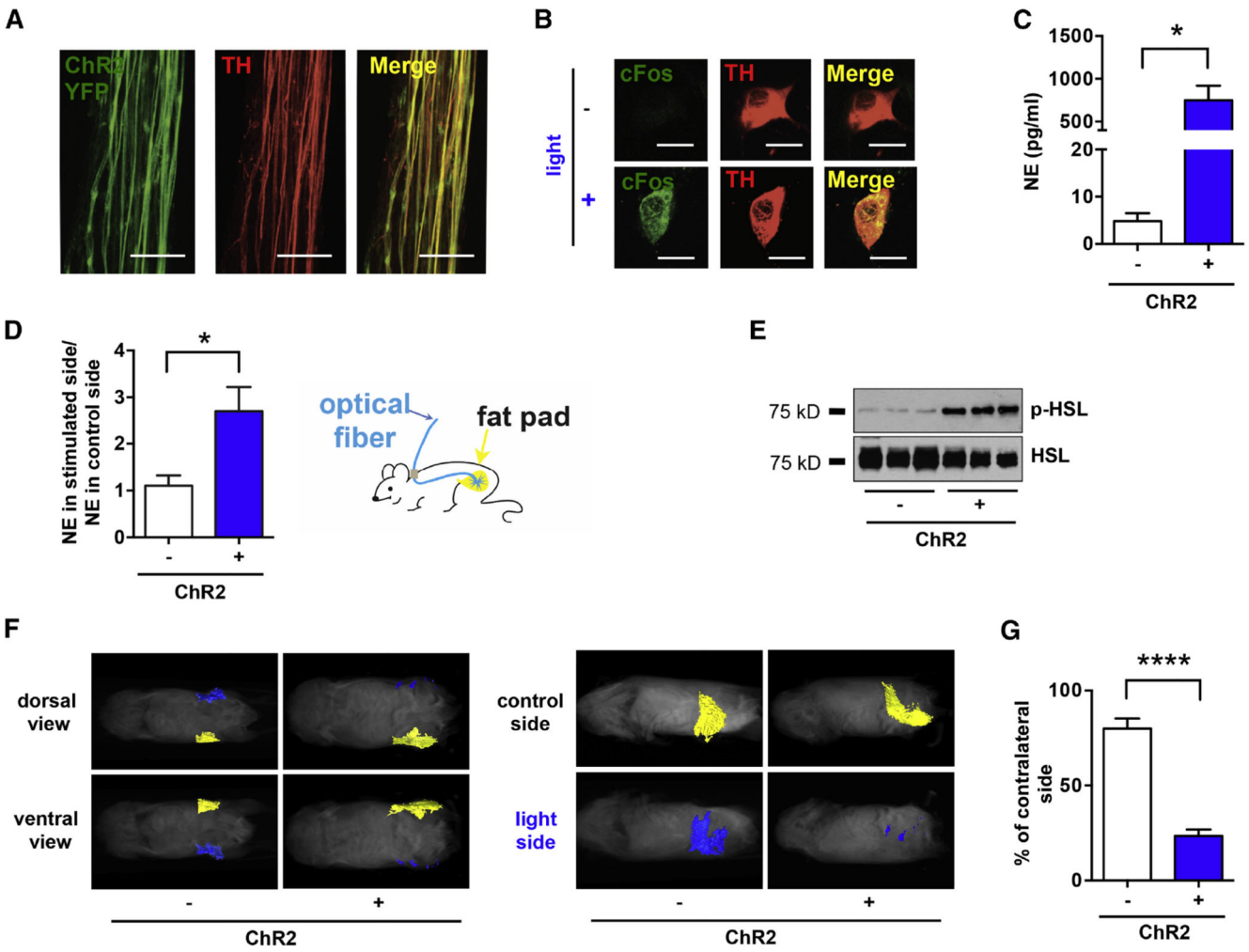

Figure 4. Optogenetic Stimulation of SNS Neurons in Fat is Sufficient to Drive Lipolysis.

(A) Complete co-localization of YFP (green) and TH (red), shown by immunohistochemistry of nerve bundles dissected from the inguinal fat pads of *TH-Cre; LSLS-ChR2-YFP*. (B) C-Fos (green) induction in cultured SNS neurons after optogenetic activation. (C) *Ex vivo* NE release upon optogenetic stimulation of sympathetic SCG explants isolated from *TH-Cre; LSL-ChR2-YFP* mice and *LSL-ChR2-YFP* control mice (*p< 0.05, n=3-6). Results are shown as mean ± SEM. (D) *In vivo* NE release in subcutaneous fat upon optogenetic stimulation of sympathetic neurons in white adipose tissues of *TH-Cre; LSL-ChR2-YFP* and *LSL-ChR2-YFP* control mice that were subcutaneously implanted with optical fibers targeting the inguinal fat pad (*p<0.05, n=8). Results are shown as mean ± SEM. (E) Immunoblot analysis of phosphorylated HSL in total protein extracts of subcutaneous fats of *TH-Cre; LSL-ChR2-YFP* and *LSL-ChR2-YFP* control mice that were subcutaneously implanted with optical fibers targeting the inguinal fat pad and optogenetically stimulated for 2 weeks (details in Experimental Procedures section). (F) MRI-guided visualization of fat in *TH-Cre; LSL-ChR2-YFP* and *LSL-ChR2-YFP* control mice that were optogenetically stimulated for 4 weeks (yellow is control inguinal fat pat, blue is light-stimulated fat pad; details in Experimental Procedures section).

(G) Quantification of fat reduction in stimulated side versus the contralateral control side (****$p<0.0001$, $n=6$). Results are shown as mean ± SEM. See also Movie S1 and S2.

Europe PMC Funders Author Manuscripts

Europe PMC Funders Author Manuscripts

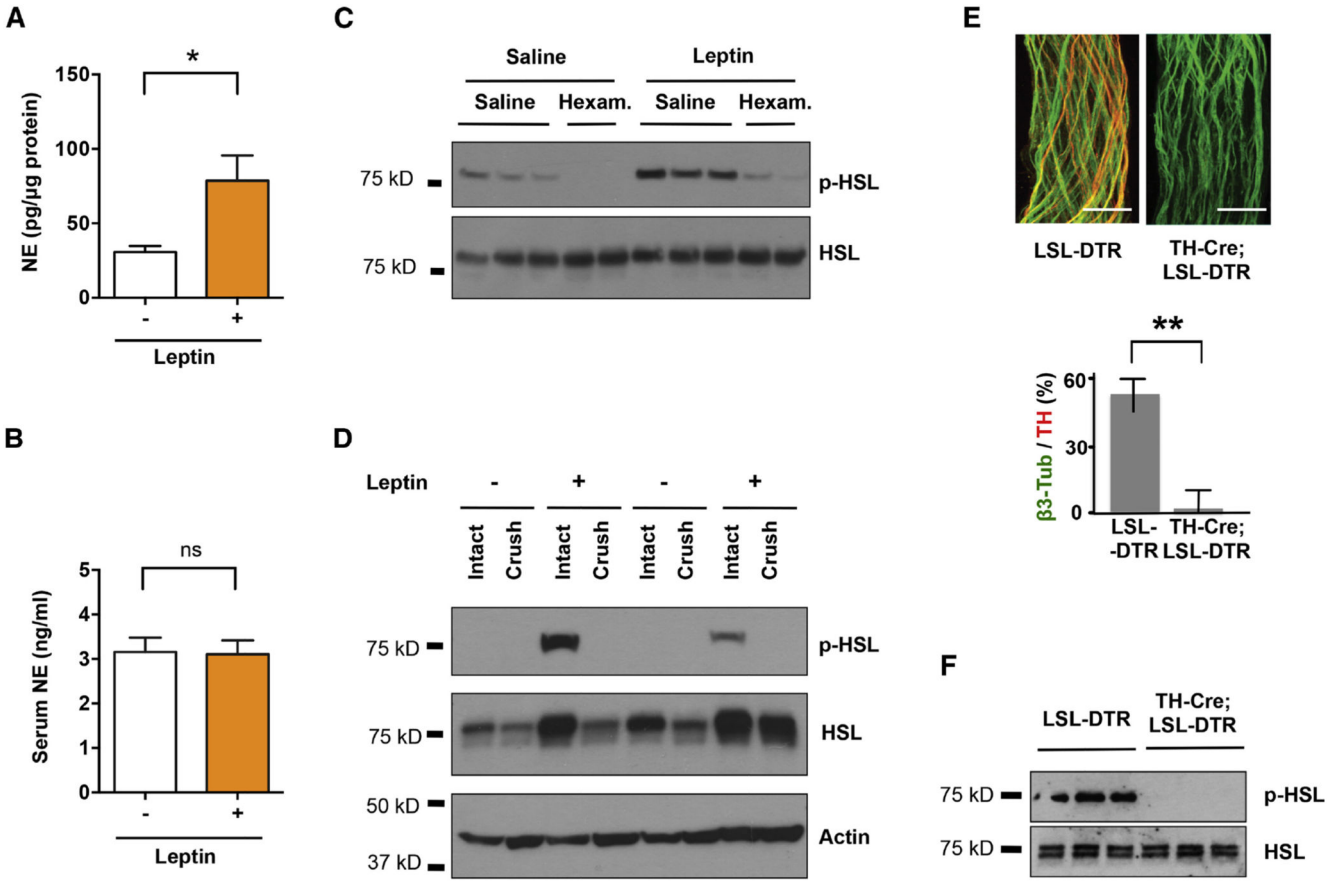

Figure 5. Sympathetic Neurons are Locally Required for Leptin-induced Lipolysis.

C57BL6/J mice were peripherally administrated with 500 ng/h recombinant leptin or saline for 2 days. (A) NE content in subcutaneous fat pads (*p<0.05, n=5) and (B) NE serum levels were measured by NE ELISA (n=4). Results are shown as mean ± SEM. C57BL6/J mice were peripherally administrated with 500 ng/h recombinant leptin at 3 days after local crush injury of nerves in fat pads. (C) Phosphorylated HSL in total protein extracts of epididymal fats were examined by immunoblot analysis. (D) Fat pads in *TH-Cre; LSL-DTR* mice were locally treated with DT. Tissue specific ablation of SNS axons confirmed by immunostaining for Tub-3 and TH (**p< 0.001, n=6). Results are shown as mean ± SEM. (E) Immunoblot analysis of phosphorylated HSL in total protein extracts of subcutaneous fats of *TH-Cre; LSL-DTR* and control mice injected with DT, following leptin treatment (500 ng/h). See also Figure S1.

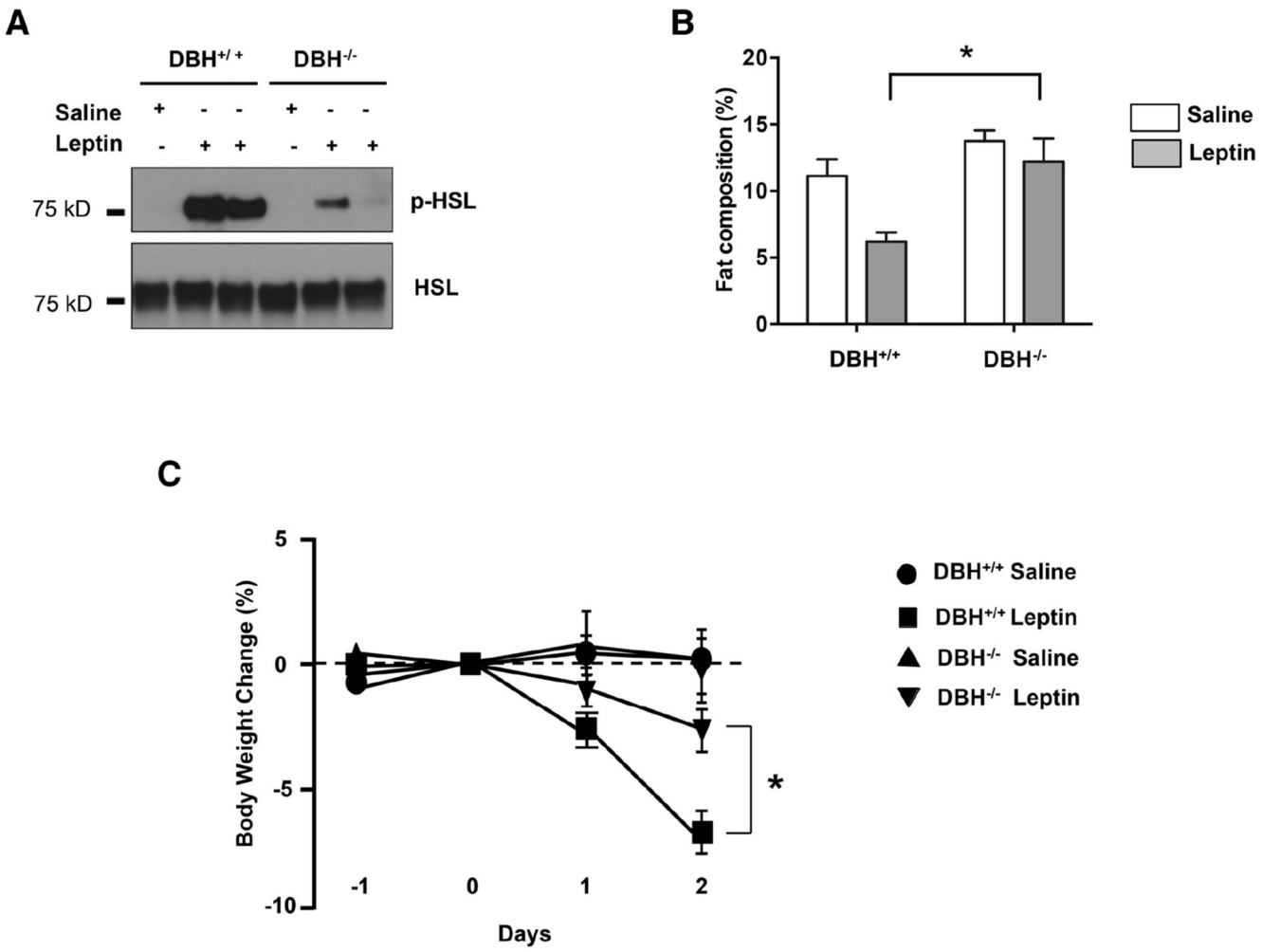

Figure 6. Norepinephrine Deficiency Impairs Leptin-induced Lipolysis.

(A) Immunoblot analysis of phosphorylated HSL in total protein extracts of fat pads of dopamine β-monoxygenase mutant and control littermates (*DBH*$^{-/-}$ and *DBH*$^{+/+}$ respectively) mice that were treated with 500 ng/h recombinant leptin. (B) Whole-body fat composition (*p< 0.05). Results are shown as mean ± SEM (n=4-5). (C) Body weight change after leptin treatment (*p< 0.05). Results are shown as mean ± SEM (n=5).

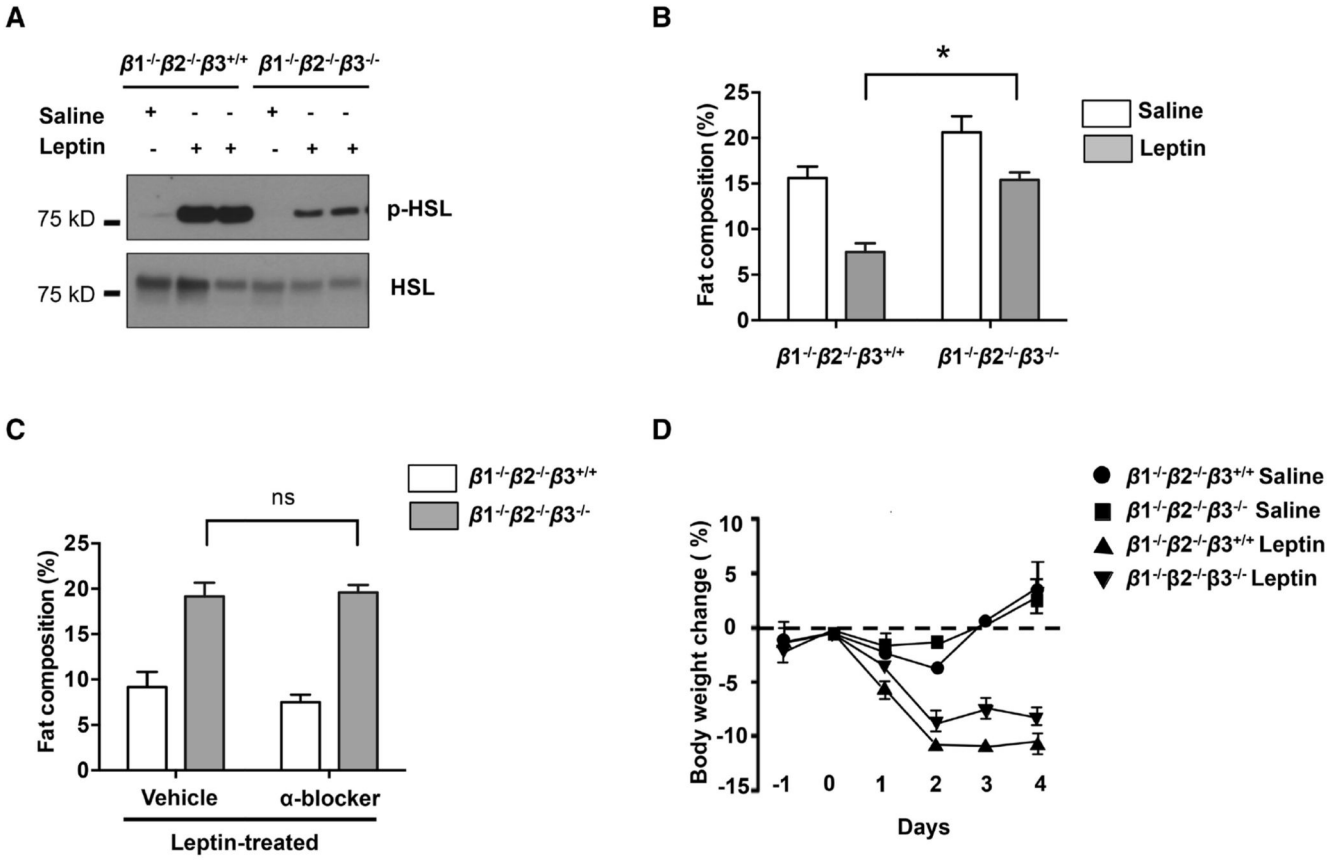

Figure 7. Deficiency of all β-adrenergic Receptors Influences Leptin--induced Lipolysis.

(A) Immunoblot analysis of phosphorylated HSL in total protein extracts of fat pads of *β1*$^{-/-}$*β2*$^{-/-}$*β3*$^{+/+}$ and *β1*$^{-/-}$*β2*$^{-/-}$*β3*$^{-/-}$ mice that were treated with 500 ng/h recombinant leptin. (B) Whole-body fat composition (*p< 0.05, n=4-5). Results are shown as mean ± SEM. (C) α-adrenergic receptors had a minor function in leptin-induced lipolysis (*p>0.05, n=4-5). Results are shown as mean ± SEM. (D) Whole-body fat composition of mice peripherally treated with recombinant leptin and α-blockers (phentolamine (5 mg/kg, IP) and phenoxybenzamine (10 mg/kg IP) was measured (n=4-5). Results are shown as mean ± SEM. See also Figure S2

Europe PMC Funders Author Manuscripts